NEW File Copy

SECURITY CLASSIFICATION OF THIS PAGE

REPORT DOCUMENTATION PAGE

Form Approved OMB No. 0704-0188

1a. REPORT SECURITY CLASSIFICATION: Unclassified	1b. RESTRICTIVE MARKINGS
AD-A219 825	3. DISTRIBUTION/AVAILABILITY OF REPORT: Unlimited
	5. MONITORING ORGANIZATION REPORT NUMBER(S): AFOSR-TR- 90-0348
6a. NAME OF PERFORMING ORGANIZATION: University of Denver (Colorado Seminary) / 6b. OFFICE SYMBOL (If applicable)	7a. NAME OF MONITORING ORGANIZATION: AFOSR/PKZ
6c. ADDRESS (City, State, and ZIP Code): Denver, Colorado 80208	7b. ADDRESS (City, State, and ZIP Code): Building 410, Bolling AFB, DC 20332-6448
8a. NAME OF FUNDING/SPONSORING ORGANIZATION: AFOSR/NC / 8b. OFFICE SYMBOL (If applicable)	9. PROCUREMENT INSTRUMENT IDENTIFICATION NUMBER: AFOSR-[redacted] 89-0018
8c. ADDRESS (City, State, and ZIP Code): Building 410, Bolling AFB, DC 20332-6448	10. SOURCE OF FUNDING NUMBERS: PROGRAM ELEMENT NO. / PROJECT NO. / TASK NO. / WORK UNIT ACCESSION NO.

11. TITLE (Include Security Classification): Informal Conference on the Chemistry of Energetic Azides, Isocyanates, and Related Species

12. PERSONAL AUTHOR(S): Robert D. Coombe

13a. TYPE OF REPORT	13b. TIME COVERED	14. DATE OF REPORT (Year, Month, Day)	15. PAGE COUNT
Final Report	FROM 88/11/1 TO _____	90/2/16	

16. SUPPLEMENTARY NOTATION

17. COSATI CODES			18. SUBJECT TERMS (Continue on reverse if necessary and identify by block number)
FIELD	GROUP	SUB-GROUP	Azides, isocyanates, nitrenes, high energy materials, lasers, spectroscopy, photochemistry, reactions

19. ABSTRACT (Continue on reverse if necessary and identify by block number)

The Informal Conference on the Chemistry of Energetic Azides, Isocyanates, and Related Species was held on the 27th and 28th of April, 1989, at the Phipps Conference Center of the University of Denver. The Conference was attended by 40 persons from academia, industry and government. 20 papers were presented on dissociation dynamics, spectroscopy and theory, and reactions of energetic azides and isocyanates.

20. DISTRIBUTION/AVAILABILITY OF ABSTRACT	21. ABSTRACT SECURITY CLASSIFICATION
☒ UNCLASSIFIED/UNLIMITED ☐ SAME AS RPT. ☐ DTIC USERS	

22a. NAME OF RESPONSIBLE INDIVIDUAL	22b. TELEPHONE (Include Area Code)	22c. OFFICE SYMBOL
Dr. F.J. Wodarczyk	(202) -767-4963	AFOSR/NC

DD Form 1473, JUN 86 — Previous editions are obsolete. — SECURITY CLASSIFICATION OF THIS PAGE

INFORMAL CONFERENCE ON THE CHEMISTRY OF

ENERGETIC AZIDES, ISOCYANATES, AND RELATED SPECIES

April 27th and 28th, 1989

Attendees

M.H. Alexander	University of Maryland
D.J. Benard	Rockwell International Science Center
Peter Bernath	University of Arizona
G. Black	SRI International
D.J. Bogan	Catholic University
N.E. Brener	Louisiana State University
M.D. Burrows	Los Alamos National Laboratory
M.A. Chowdhury	Rockwell International Science Center
D.B. Clark	University of Denver
R.A. Conklin	University of Denver
R.D. Coombe	University of Denver
P.J. Dagdigian	Johns Hopkins University
L.P. Davis	AFOSR
E.A. Dorko	Air Force Weapons Laboratory
T. Fueno	Osaka University
J.V. Gilbert	University of Denver
T.L. Henshaw	F.J. Seiler Research Laboratory/USAFA
J.W. Hudgens	National Institute of Standards and Technology

Informal Azide Conference
List of Attendees

R.C. Jenson	Hercules, Inc.
N.R. Kestner	Louisiana State University
W.J. Kessler	Physical Sciences, Inc.
J.B. Koffend	Aerospace Corp.
S.R. Leone	University of Colorado/JILA
X. Liu	University of Denver
N.H. Machara	University of Denver
W.J. Marinelli	Physical Sciences, Inc.
H.H. Michels	United Technologies Research Center
W.L. Nicolai	Hercules, Inc.
A.P. Ongstad	F.J. Seiler Research Laboratory/USAFA
G.P. Perram	Air Force Weapons Laboratory
S.L. Rodgers	Air Force Astronautics Laboratory
S. Rosenwaks	Ben-Gurion University
L.A. Schlie	Air Force Weapons Laboratory
T.A. Seder	Rockwell International Science Center
D.W. Setser	Kansas State University
D.H. Stedman	University of Denver
W.G. Thorpe	F.J. Seiler Research Laboratory/USAFA
B.K. Winker	Rockwell International Science Center
F.J. Wodarczyk	AFOSR
C.H. Wu	Naval Research Laboratory

INFORMAL CONFERENCE ON THE CHEMISTRY OF

ENERGETIC AZIDES, ISOCYANATES, AND RELATED SPECIES

April 27th and 28th, 1989

Phipps Conference Center, University of Denver

Denver, Colorado

Thursday, April 27th

8:00 AM — Bus from Writers' Manor to Phipps Conference Center

8:15 - 8:45 — Continental Breakfast

8:45 - 9:00 — Welcome. R.D. Coombe and F.J. Wodarczyk

Session I. Dissociation Dynamics

Chairman: D.J. Benard (Rockwell International)

1. 9:00 - 9:30 — "Model Studies of CBES Decomposition," T.A. Seder and D.J. Benard (Rockwell International Science Center)

2. 9:30 - 10:00 — "Production of NF($a^1\Delta$) by Dissociation of Fluorine Azide," B.K. Winker and D.J. Benard (Rockwell International Science Center)

3. 10:00 - 10:30 — "Ab Initio Study of the Energetics of the Decomposition of HN_3 and N_3," M.H. Alexander (University of Maryland)

10:30 - 10:45 — Break

4. 10:45 - 11:15 — "A Shock Tube Study of HNCO Decomposition," C.H. Wu, H-T. Wang, and M.C. Lin (Naval Research Laboratory), and R.A. Fifer (Army Ballistic Research Laboratory)

5. 11:15 - 11:45 — "Plasma Breakdown Behavior of Hydrogen Azide (HN_3) Gas Mixtures," L.A. Schlie, M.D. Wright, and C.A. Denman (Air Force Weapons Laboratory)

6. 11:45 - 12:15 — "Photodissociation of NCO Radicals," X. Liu and R.D. Coombe (University of Denver)

INFORMAL AZIDES CONFERENCE - SCHEDULE
April 27th and 28, 1989

12:15 - 1:30 Lunch

Session II. Spectroscopy and Theory

Chairman: D.W. Setser (Kansas State University)

7. 1:30 - 2:00 "Laser and Fourier Transform Spectroscopy of Energetic Species," Peter Bernath (University of Arizona)

8. 200 - 2:30 "Detection of the Azide Radical by REMPLI Spectroscopy," J.W. Hudgens and R.D. Johnson, III (National Institute of Standards and Technology)

9. 2:30 - 3:00 "Theoretical Studies of Halogen Azides and Azide - Like Structures," H.H. Michels and J.A. Montgomery, Jr. (United Technologies Research Center)

3:00 - 3:15 Break

10. 3:15 - 3:45 "Theoretical Studies of FN_3 Clusters," N.E. Brener, J. Callaway, N.R. Kestner, and H. Chen (Louisiana State University).

11. 3:45 - 4:15 "Theoretical Studies of Fluorine Azide in the Gas Phase and on surfaces," N.R. Kestner, N.E. Brener, and J. Callaway (Louisiana State University)

Bus to Writer's Manor

Friday, April 28th

8:00 Bus from Writer's Manor to Phipps Conference Center

8:15 - 8:45 Continental Breakfast

Session III. Reactions I

Chairman: G. Black (SRI International)

INFORMAL AZIDES CONFERENCE - SCHEDULE
April 27th and 28th, 1989

13. 8:45 - 9:15 "Mechanisms of the Gas-Phase Decompositions of HN_3 and HNCO in the Presence of NO and O_2," Takayuki Fueno (Osaka University)

14. 9:15 - 9:45 "Isocyanic Acid as a Laser Fuel," M.A. Chowdhury and D.J. Benard (Rockwell International Science Center)

15. 9:45 - 10:15 "Experimental Study of Dynamical Processes on HN_3 Potential Energy Surfaces: The H + N_3 Reaction, Photodissociation of HN_3, and Quenching of NH ($a^1\Delta$) by N_2," P.J. Dagdigian (Johns Hopkins University)

10:15 - 10:30 Break

16. 10:30 - 11:00 "Chemiluminescent Reactions of Group VI Atoms with Azide Radicals," T.L. Henshaw, A.P. Ongstad, and R.I. Lawconnell (Frank J. Seiler Research Laboratory, U.S. Air Force Academy)

17. 11:00 - 11:30 "Chemiluminescent Reactions of Azide Radicals," W.J. Marinelli and W.J. Kessler (Physical Sciences, Inc.)

11:30 - 12:30 Lunch

Session IV Reactions II

Chairman: R.D. Coombe (University of Denver)

18. 12:30 - 1:00 "Hydrazoic Acid as an Analytical Reagent," D.H. Stedman and M.R. Burkhardt (University of Denver)

19. 1:00 - 1:30 "Electronic Excitation of Pb Atoms Following Detonation of Lead Azide," I. Bar, A. Ben-Tov, Z. Ben-Parath, D. Heflinger, Y. Kaufman, C. Miron, M. Sapir, Y. Tzuk, and S. Rosenwaks (Ben-Gurion University)

20. 1:30 - 2:00 "NO (A ---> X) and N_2 (C ---> B) Laser Experiments," M.D. Burrows, R.F. Shea, and G.W. York (Los Alamos National Laboratory)

2:15 Adjourn

2:30 Bus to Writers' Manor

INFORMAL CONFERENCE ON THE CHEMISTRY OF ENERGETIC AZIDES, ISOCYANATES, AND RELATED SPECIES

UNIVERSITY of DENVER

APRIL 27TH AND 28TH, 1989

PHIPPS CONFERENCE CENTER, UNIVERSITY OF DENVER

DENVER, COLORADO

Model Studies of CBES Decomposition

T. A. Seder and D. J. Benard
Rockwell International Science Center
Thousand Oaks, CA 91360

Materials having large positive heats of formation, such as FN_3 ($\Delta H_f \sim 130$ kcal/ mol), are potentially useful as advanced propellants. However, because of their exceedingly fragile nature and high energy content, these materials readily exhibit shock induced detonation. Thus, prior to device application, these materials must be stabilized and their burn rates moderated by, perhaps, incorporating additives into the propellant.

At Rockwell Science Center we are currently studying the decomposition physics of laser ignited cryogenic films of FN_3. To date we have characterized the emissions appearing upon ignition of the condensed phase material. Contrary to the decomposition of gas phase FN_3, no emission from the ($a^1\Delta$) or the ($b^1\Sigma$) states of the NF fragment are observed. Only a temporally complex band, centered at 450 nm and appearing on a 10 us time scale, is observed in the emission spectrum. The emitting species is as yet unidentified.

We have also measured the burn rate of the material by recording the time required for the decomposition front to propogate from the ignition site to a distant scattering probe. Our results indicate that pure FN_3 films burn at a rate of 1 mm/ us. Also, this rate can be reduced by incorporating additives such as SF_6 or NF_3 into the film.

In addition to the above results, recent experiments to image the plume of product gases at various times following ignition via Schlieren photography will be discussed. The techniques developed at the Science Center for the safe production and handling FN_3 will also be presented.

PRODUCTION OF NF($a^1\Delta$) BY DISSOCIATION OF FLUORINE AZIDE

B. K. Winker and D. J. Benard
Rockwell International Science Center
Thousand Oaks, California 91360

The thermal dissociation of FN_3 has been investigated using pulsed laser thermolysis with HF, DF, and CO_2 lasers. The disappearance of FN_3 was monitored by ultraviolet absorption at 210 nm. The production of NF($a^1\Delta$) was monitored by absolute photometry on the NF(a-X) transition at 874 nm.

In the case of HF/DF, mixtures of FN_3, HF or DF, and He were irradiated with a pulsed TEA HF or DF laser. Absorption of ca. 5% of the laser pulse by HF or DF resulted in vibrational excitation in levels v"=1-3. Reactions of vibrationally excited HF or DF molecules with FN_3 were found to dissociate the azide, but not to yield metastable NF. Subsequent heating of the gas due to partial dissociation of FN_3 induced the remaining FN_3 to dissociate thermally, resulting in efficient production of NF($a^1\Delta$). The activation energy for thermal dissociation of FN_3 was obtained and it agrees with *ab initio* calculations by Michels.

In the case of CO_2, mixtures of FN_3, SF_6, and He were irradiated with a pulsed TEA CO_2 laser. Absorption of ca. 30% of the laser pulse by SF_6 resulted in rapid heating of the gas mixture to temperatures of 950-1200 K. Subsequent thermal dissociation of FN_3 produced NF($a^1\Delta$) with near unity yield. Concentrations of NF($a^1\Delta$) as high as $10^{16}/cm^3$ were obtained and the decay of NF($a^1\Delta$) was dominated by self-annihilation. The rate of NF($a^1\Delta$) self-quenching was found to be $3 \times 10^{-12} cm^3/s$, in good agreement with previous flowtube studies by Setser.

AB INITIO STUDY OF THE ENERGETICS OF THE DECOMPOSITION OF HN_3 AND N_3

Millard H. Alexander, Department of Chemistry, University of Maryland, College Park, MD 20742

We shall report on an investigation of the energetics of the dissociation of ground state hydrazoic acid HN_3 and the azide radical N_3. The study is limited to decomposition on the lowest potential energy surface, namely

$$HN_3(\tilde{X}\,^1A') \rightarrow N_2(X^1\Sigma_g^+) + NH(a^1\Delta) \quad (1)$$

$$\rightarrow N_3(\tilde{X}\,^2\Pi_g) + H(^2S) \quad (2)$$

$$N_3(\tilde{X}\,^2\Pi_g) \rightarrow N_2(X^1\Sigma_g^+) + N(^2D) \quad (3)$$

and to the lowest spin-forbidden decomposition channel

$$HN_3(\tilde{X}\,^1A') \rightarrow N_2(X^1\Sigma_g^+) + NH(X^3\Sigma^-) \quad (4)$$

$$N_3(\tilde{X}\,^2\Pi_g) \rightarrow N_2(X^1\Sigma_g^+) + N(^4S)\ . \quad (5)$$

Processes (1) and (4) are under experimental investigation by King, Stephenson, and co-workers at NIST.[1,2,3] The relative enthalpies for dissociation of HN_3 to $NH+N_2$ [Eqs. (1) and (2)] or to the other spin-allowed product channel (3) will play an important role in determining the relative branching ratios in the uv dissociation of HN_3, as well as controlling the exothermicity of the abstraction reaction

$$H(^2S) + N_3(\tilde{X}\,^2\Pi_g) \rightarrow NH(X^3\Sigma^-, a^1\Delta) + N_2(X^1\Sigma_g^+)\ , \quad (6)$$

now under study in Dagdigian's laboratory.

Complete active space SCF and multireference configuration interaction calculations with large basis sets have been used (a) to determine the bond dissociation energies of HN_3 and N_3, (b) to locate the geometry and topology of the transition state for spin-forbidden decomposition and the corresponding activation energy, and (c) to investigate the magnitude and origin of exit channel barriers in the spin-allowed decomposition channel.[4,5] The barrier to the spin-

---

[1] B. R. Foy, M. P. Casassa, J. C. Stephenson, and D. S. King, J. Chem. Phys., 89, 608 (1988).

[2] J. C. Stephenson, M. P. Casassa, and D. S. King, J. Chem. Phys. 89, 1378 (1988).

[3] B. Foy, M. P. Casassa, J. C. Stephenson, and D. S. King, J. Chem. Phys., submitted.

[4] M. H. Alexander, H.-J. Werner, and P. J. Dagdigian, J. Chem. Phys. 89, 1388 (1988).

[5] M. H. Alexander, T. Hemmer, H.-J. Werner, and P. J. Knowles, J. Chem. Phys., submitted; M. H. Alexander, H.-J. Werner, and P. J. Knowles, manuscript in preparation.

forbidden decomposition of HN_3 [Eq.(4)], including zero-point corrections is predicted to be E_a =193 kJ/mol (16,152 cm^{-1}). This value is in good agreement with the HN_3 decomposition lifetimes seen in the overtone pumping experiments of King, Stephenson, Casassa, and Foy at NIST,[1,3] which indicate that E_a = lies between 15,000 cm^{-1} and 17,700 cm^{-1}, but considerably larger than the earlier experimental activation energies (116 – 165 kJ/mol) derived from shock tube decomposition experiments.[6]

The dependence on internal coordinates of the potential energy surface of HN_3 in the region of the singlet-triplet crossing is illustrated by the following surface projection plots.

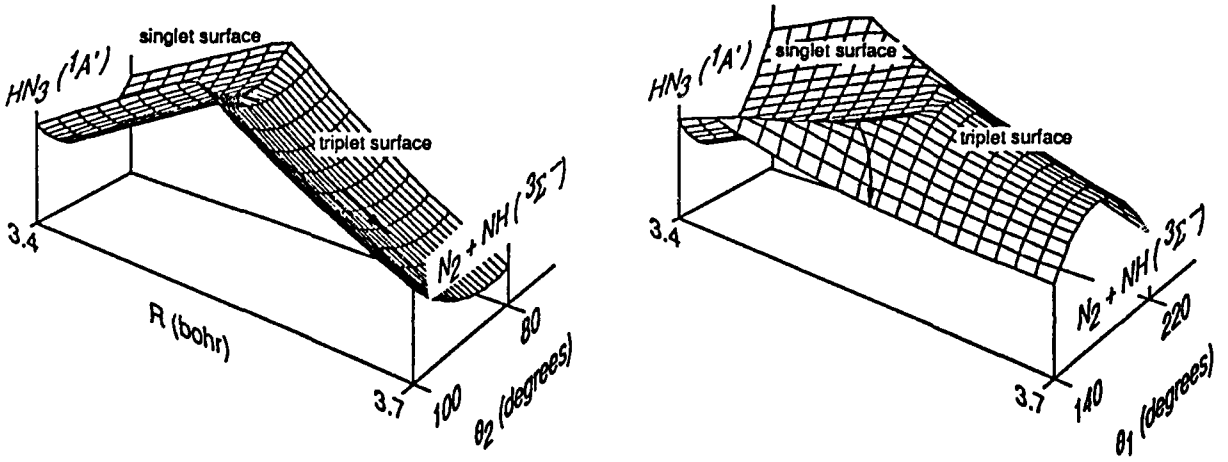

Dependence of the energy of the HN_3 molecule on the NNH angle (left panel) and the NNN angle (right panel) as a function of the NN–NH distance in the region of the singlet-triplet crossing. The arrows indicate the steepest descent path beyond the saddle point.

As can be seen clearly in these two plots, decomposition should result in rotationally cold $NH(X^3\Sigma^-)$ products, as seen experimentally,[1,2] but could well lead to rotationally hotter N_2 fragments. Perhaps this could be studied with REMPI detection.

The calculated enthalpy of decomposition of HN_3 is 25–40 kJ/mol, in good agreement with the experimental estimate of 46 kJ/mol.[7]

In the spin-allowed (singlet) decomposition channel [Eq. (1)] our calculations indicate the

[6] O. Kajimoto, T. Yamamoto, and T. Fueno, J. Phys. Chem. 83, 429 (1979); C. Paillard, G. Dupré, and J. Combourieu, J. Chim. Phys. 82, 489 (1985).

[7] H. Okabe and M. Lenzi, J. Chem. Phys. 47, 5241 (1967).

existence of a small barrier of height 1000 – 1500 cm^{-1}. This barrier can be attributed to orbital constriction: as the N_2–NH distance decreases, Pauli repulsion with the lone-pair σ orbital on the N_2 forces one of the NH π orbitals out of the occupied space. This calculated barrier is consistent with the observation by King, Casassa, and Stephenson[2] of a hyperthermal ($E_{tr} \approx 1700$ cm^{-1}) translational energy of the nascent NH($a^1\Delta$) products in the irmpd decomposition of HN_3. Also, a small barrier is consistent with the observed small rate constant for quenching of NH($a^1\Delta$) by N_2.[8] In the absence of a barrier, quenching should be efficient, mediated by approach on the singlet surface followed by crossing to the triplet surface, as proposed some time ago by Fisher and Bauer[9] as the quenching mechanism in the isoelectronic O(^{1}D)+N_2 system.

In the case of N_3 the calculated barrier to spin-forbidden decomposition [Eq. (5)] is predicted to be 212–215 kJ/mol, slightly higher than the comparable barrier in HN_3 and considerably higher than the early experimental estimate[10] of 59 – 130 kJ/mol, derived from studies of the kinetics of the isotopic substitution reaction $^{15}N + N_2 \rightarrow {}^{14}N^{15}N + {}^{14}N$. The N–NN bond dissociation energy in N_3 is predicted to be 3–12 kJ/mol, much less than the experimental estimate of 53.9 ± 20.9 kJ/mol obtained using the JANAF[11] value of the heat of formation of N_3 (417.0 ± 20.9 kJ/mol). However, our estimate of the N–NN bond dissociation energy is consistent with the value of 2.2± 20.9 kJ/mol which is obtained with the larger heat of formation of N_3 (468.6 ± 20.9 kJ/mol) advocated by Brauman and co-workers[12].

As in the case of HN_3 there also exists a slight barrier in the exit channel for the spin-allowed decomposition of N_3 leading to N(^{2}D) products [Eq. (3)]. This barrier would explain why the observed rate for the thermal quenching of N(^{2}D) by N_2 ($k_q = 1.85 \pm 0.15 \cdot 10^{-14}$ cm^3/molecule·s [13]) is more than two orders of magnitude slower than that of O(^{1}D) by N_2 ($k_q = 5.5 \cdot 10^{-11}$ cm^3/molecule·s [14]).

---

[8] F. Freitag, F. Rohrer, and F. Stuhl, J. Phys. Chem., in press.

[9] E. R. Fisher and E. Bauer , J. Chem. Phys. 57,, 1966 (1972).

[10] R. A. Back and J. Y. P. Mui, J. Phys. Chem. 66, 1364 (1962).

[11] JANAF Thermochemical Tables, 3rd edition, 1985.

[12] M.J. Pellerite, R. L. Jackson, and J. I. Brauman, J. Phys. Chem. 85, 1624 (1981); E. Illenberger, P. B. Comita, J. I. Brauman, H. P. Fenzlaff, M. Heni, N. Heinrich, W. Koch, G. Frenking, Ber. Bunsen-Ges. Phys. Chem. 89, 1026 (1985).

[13] T. G. Slanger and G. Black, J. Chem. Phys. 64, 4442 (1976).

[14] T. G. Slanger and G. Black, J. Chem. Phys. 60, 468 (1974).

A Shock Tube Study of HNCO decomposition

C.H.Wu[a], H.-T. Wang, and M.C. Lin[b]
Chemistry Division, Code 6100, Naval Research Laboratory
Washington, DC 20375-5000
and
R. A. Fifer
Interior Ballistic Division, SLCBR-IB-I,
Army Ballistic Research Laboratory
Aberdeen Proving Ground, MD 21005-5066

The thermal decomposition of HNCO (isocyanic acid, 0.2% and 0.5% in Ar) has been studied behind incident shock waves over the temperature range 2100-2500 K and pressures between 0.3 and 0.6 atm. The concentration profiles of CO were monitored using a frequency-stabilized CW CO laser at (V=2 to V=1 P(10). The initial step of decomposition was shown to be HNCO + Ar ---> NH + CO + Ar with the rate constant $k = 10^{16.28}\exp[-(90.0)\ \text{kcal/mol/RT}]\ \text{cm}^3\text{mol}^{-1}\text{s}^{-1}$.

The HNCO decomposition is also being studied in another shock tube at the BRL using Lyman-alpha absorption methods to monitor H-atom concentration profiles for dilute mixtures (100-500 ppm) of HNCO in Ar. The branching ratio of the two pathways

$$\text{HNCO} + \text{Ar} \text{ ---> } \text{NH} + \text{CO} + \text{Ar} \qquad (1)$$
$$\text{HNCO} + \text{Ar} \text{ ---> } \text{H} + \text{NCO} + \text{Ar} \qquad (2)$$

is being determined at high temperature. Because the potential importance of H atoms as chain carriers in the subsequent reaction HNCO + NO, it is essential to understand the contribution of reaction 2 to the thermal De-NO_x process.

The experimental data were kinetically modeled using suitable reaction mechanisms involving HNCO and related N-containing radicals such as NH, NH_2, and NCO. Sensitivity analyses are also performed to determine the importance of each elementary reaction in the reaction process.

a. ONT postdoctoral associate
b. Department of Chemistry, Emory University, Atlanta, GA 30322.

Plasma Breakdown Behavior of Hydrogen Azide (HN_3) Gas Mixtures†

L. A. Schlie, M. W. Wright, and C. A. Denman

Advanced Laser Technology Division
Air Force Weapons Laboratory (AFWL/ARDI)
Kirtland AFB, N.M. 87117–6008

The highly energetic azide gases (8.5 MJ/KG) have recently received much attention as potential high energy lasers. Most investigators, however, have addressed only the chemical reactions and the resultant yields of the N_2(A,B,C) states. As an alternative to just chemical use of azides for lasers, hybrid electro–chemical laser systems in the ultraviolet/visible region offer much potential. Such a concept utilizes plasma processes to initiate and sustain the chemical reactions necessary to produce the required inversions. Plasma initiated processes in hydrogen azide (HN_3) seem particularly useful in the development of azide based lasers.

Recent work on electron beam initiated plasma studies have shown that HN_3 is a strong electron attaching molecule. In an attempt to better understand the plasma transport properties of this particular azide gas, the electrical breakdown behavior of HN_3 was investigated. Surprisingly, there was a marked difference in the breakdown phenomena for different pressures of buffer gases. With HN_3 pressures of a few torr mixed with an atm. of inert gas, the plasma breakdown constituency of the original species is retained. In pure hydrogen azide gas, its breakdown *creates a chain chemical reaction* producing very intense N_2 first and second positive band emission. In addition, such a breakdown causes the molecular constituency of the gas to change from HN_3 to only H_2 and N_2, as determined by a mass spectrograph. Upon completion of the plasma initiated chain reactions, a factor of two pressure increase is always observed due to the stoichiometry of the pertinent reactions. The transient spectral behavior elucidates the kinetic processes occurring in this gas. The effect of gas temperature on the kinetics of this system is discussed. Finally, the implication of such plasma breakdown processes on potential hybrid electro–chemical lasers will be described.

†Supported by the Air Force Office of Scientific Research (AFOSR), Bolling AFB, D.C.

PHOTODISSOCIATION OF NCO RADICALS

X. Liu and R.D. Coombe

Department of Chemistry, University of Denver

Denver, Colorado 80208

Photolysis of NCO ($X^2\Pi$) radicals at 193 nm leads to the production of $O(^3P)$ and $CN(X^2\Sigma^+)$ fragments. The CN(X) was detected by laser-induced fluorescence on the $X^2\Sigma^+ \dashrightarrow B^2\Sigma^+$ transition near 389 nm. The internal energy distribution in the CN fragment was determined by simulation of experimental LIF excitation spectra. The vibrational distribution obtained from this procedure was v=0: v=1: v=2: v=3 = 0.43: 0.32: 0.21: 0.04. The rotational population distribution could not be described by a Bolzmann equilibrium temperature, but rather was well fit by a bi-modal distribution comprised of relaxed and unrelaxed components extending to very high J. These data suggest that the excited dissociative state pumped by the 193 nm radiation has a bent configuration. From the internal energy distributions in the CN fragment, a lower limit for the heat of formation of NCO, $\Delta H_{f,298} \geq 40.7$ kcal/mole, was determined.

The 193 nm photolysis also produces prompt emission from the NCO radicals themselves in the region 340 - 420 nm. Preliminary analysis of the spectrum of this emission indicates a transition from a high lying excited state to the $A^2\Sigma^+$ state. The upper state of this transition is apparently not the same as that which dissociates to O + CN, but rather has a linear configuration.

Laser and Fourier Transform Spectroscopy of Energetic Species

by

Peter Bernath
Department of Chemistry
University of Arizona
Tucson, AZ 85721

We have discovered that Ca and Sr vapors react with HN_3 and HNCO to give MN_3 and MNCO (M = Ca and Sr) molecules. These molecules proved to be linear and N-bonding. Low-resolution spectra and high-resolution analyses of the $\tilde{A}^2\Pi - \tilde{X}^2\Sigma^+$ transitions of SrNCO and SrN_3 will be presented.[1,2] C.W. dye laser methods provided the necessary sensitivity and resolution for the analyses. These molecules are the first gas-phase metal azides and isocyanates to be spectroscopically characterized.

The high-resolution infrared absorption spectrum of the ν_3 mode of N_3 was recorded.[3] N_3 was synthesized by the reaction of Cl atoms and HN_3 in a long path cell. The frequency of the ν_3 mode at 1645 cm^{-1} was found to be somewhat lower than expected.

Recently we recorded the ultracold electronic emission spectrum of CCN. The $\tilde{A}^2\Delta - \tilde{X}^2\Pi$ transition was observed with a high-resolution Fourier transform spectrometer. An Engelking type[4] of free radical jet source using diazoacetonitrile ($HC(N_2)CN$) in helium provided CCN emission.

Finally, if time permits, I will discuss our observations of the high-resolution infrared spectra of C_3[5] and C_5 in a carbon star.

References

1. C.R. Brazier and P.F. Bernath, Laser Spectroscopy of Calcium and Strontium Monoazide Free Radicals, *J. Chem. Phys.* **88**, 2112-2116 (1988).

2. L.C. O'Brien and P.F. Bernath, High-Resolution Laser Spectroscopy of Strontium Isocyanate, SrNCO, *J. Chem. Phys.* **88**, 2117-2120 (1988).

3. C.R. Brazier, P.F. Bernath, J.B. Burkholder and C.J. Howard, Fourier Transform Spectroscopy of the ν_3 Band of the N_3 Radical, *J. Chem. Phys.* **89**, 1762 (1988).

4. P. Engelking, *Rev. Sci. Instrum.* **57**, 2274-2277 (1986).

5. K.H. Hinkle, J.J. Keady and P.F. Bernath, Detection of C_3 in the Circumstellar Shell of IRC+10216, *Science* **241**. 1319-1322 (1988).

DETECTION OF THE AZIDE RADICAL WITH REMPI SPECTROSCOPY

Jeffrey W. Hudgens and Russell D. Johnson III
Chemical Kinetics Division
Center for Chemical Technology
National Institute of Standards and Technology(c
Gaithersburg, MD 20899

We have conducted experiments to observe resonance enhanced multiphoton ionization spectra of the azide radical. Azide radicals were produced in a flow reactor by the reaction of HN_3 with fluorine atoms. A portion of the reactor effluent flowed into a time-of-flight mass spectrometer and was irradiated with focused light produced by a tuneable dye laser. The wavelength range from 222-500 nm was searched. A weak band system carried by N_3^+ (m/z 42) was observed between 333-337 nm. Chemical studies showed this system to arise from N_3 radicals. Nonresonant multiphoton ionization of HN_3 (m/z 43) was also observed between 334-347 nm. The REMPI spectrum of NH radicals produced by photodissociation of HN_3 was also observed between 260-270 nm.

PHOTOELECTRON SPECTROSCOPY OF ALIPHATIC AZIDES

M.L. Costa[*], M.A. Almoster Ferreira[≠*] and B.J. Costa Cabral[≠∇]

[*]Center for Mass Spectrometry of the University of Lisbon
Complexo I (INIC), Av. Rovisco Pais, 1096 Lisboa, Codex, Portugal

[≠]University of Lisbon, Faculty of Sciences, Department of Chemistry,
Rua Ernesto de Vasconcelos, Edifício C1, 1700 Lisboa, Portugal

[∇]Center for Physics of the Condensed Matter, Complexo II (INIC),
Av. Prof. Gama Pinto, nº 2, 1699 Lisboa, Portugal

Ultraviolet Photoelectron Spectroscopy (UVPES) has been generally employed to study valence orbital structure of molecules and ions (1, 2).

The outstanding feature of UVPES is its ability to eject electrons from any of the occupied energy levels in a molecule and, since each of these levels has a different ionization energy, only those particlar electrons for study are selected. According to Koopmans' theorem (3), each ionization energy is simply equal in magnitude to an orbital energy. Through use of this approximation, UVPES provides an experimental determination of a molecular orbital diagram.

Ab-initio calculations for ethyl azide-$CH_3CH_2N_3$ - azidoacetone -$CH_3COCH_2N_3$-, and azidoethanol-$CH_2OHCH_2N_3$- were performed, using the GAUSSIAN 82 (4) computer program at the 4-31G, 4-31G** and 6-31G+ basis set level, with the aim of interpreting their ultraviolet photoelectron spectra, as part of a general research-project into open-chain aliphatic azides.

The first bands of the photoelectron spectra of the azides under study are intense and sharp indicating ionization from a non-bonding orbital. This is in accordance with the performed calculations, which also predict a non-bonding character to the molecular orbitals corresponding to the first ionization energies. Good agreement was also found when comparing the second ionization energies given by the calculations with the second bands of the photoelectron spectra of the molecules.

Using this spectroscopic technique the decomposition by pyrolysis of these compounds was investigated and the possible pyrolysis products analised.

In situ mass analysis of the ions produced in the ionization region

was expected to be of great value in the interpretation of the photoelectron spectra.

The apparatus used for this study was a photoelectron spectrometer modified to permit the instrument to be used as a photoion mass analyser (5).

The photoelectron spectra were recorded first at room temperature together with the photoion mass spectra, followed by the calibration. The temperature of the reactor was then increased and this operation was repeated.

The mass spectra were calibrated with the mixture CS_2/CH_3I which provides peaks at masses covering a convenient range (44-142 a.m.u).

BIBLIOGRAFIA

(1) - D.W. Turner, C. Baker, A.D. Baker and C.R. Brundle, "Molecular Photoelectron Spectroscopy", Wiley-Interscience, 1970.

(2) - K. Kimura, S. Katsumata, Y. Achiba, T. Yamazaki, S. Iwata, "Handbook of HeI Photoelectron Spectra of Fundamental Organic Molecules", Halsted Press, New York, 1981.

(3) - T. Koopmans, Physica 1, 104 (1933).

(4) - J.S. Binkley, M.J. Frisch, D.J. DeFrees, K. Rahgavachari, R. A. Whiteside, H.B. Schlegel, E.M. Fluder and J.A. Pople, GAUSSIAN 82, Department of Chemistry, Carnegie-Mellon University, Pittsburg, 1982.

(5) - M.L. Costa, in J.F.J. Todd (Editor), "Advances in Mass Spectrometry", vol. 10, John Wiley & Sons, N.Y., 1339, 1986.

Theoretical Studies of Halogen Azides and Azide-Like Structures

H. H. Michels and J. A. Montgomery, Jr.
United Technologies Research Center
East Hartford, CT 06108

Calculations of hydroazoic acid (HN_3), fluorine azide (FN_3), fluorine isocyanate (FNCO), asymmetric dinitrogen dioxide (a-N_2O_2) and difluoraminoborane (FNBF) have been carried out at several levels of theory to determine the most stable geometries of these azides and azide-like compounds. The results are summarized in Table 1 which indicate that a stable C_s structure exists for each of these compounds. A vibrational frequency analysis has also been carried out for each of these compounds. The results indicate a stable structure in $^1A'$ symmetry. A comparison with experimentally determined structures for HN_3 [1], FN_3 [2] and FNCO[3] has been made. It is clear that very good agreement has already been achieved at the MP2 level of theory.

a-N_2O_2

The most significant result of our studies of azide-like structures is the prediction of a stable, asymmetric C_s structure of dinitrogen dioxide, in $^1A'$ symmetry, with a characteristic IR frequency of 1206 cm^{-1}, corresponding to the N-O stretch. This frequency has previously been reported by Milligan and Jacox[4] in argon matrix studies of irradiated N_2O in the presence of alkali atoms and assigned to a possible N_2O_2 anion. It is not characteristic of other known nitrogen oxides. The calculated geometry for a-N_2O_2 is very similar to the structures of the isoelectronic species FN_3 and FNCO.

There are also low-lying tiplet states of N_2O_2 arising from $O[^3P] + N_2O$ and $O_2[^3\Sigma_g^-] + N_2$, and it is necessary to know their location to assess the stability of the singlet. A CISD/6-31G* energy calculation on the lowest $^3A''$ state, performed at the optimized geometry of the singlet, shows that the triplet lies 67 kJ/mol higher than the singlet. Since asymptotically the triplet surface lies lower than the singlet, further calculations are underway to characterize the crossing region and its effect on the stability of singlet a-N_2O_2.

The transition state of a-N_2O_2 corresponds to the activation energy required to decompose a-N_2O_2 into $O_2[a^1\Delta_g] + N_2[X^1\Sigma_g^+]$. The geometry corresponding to the transition state is: R_{OO} = 1.3980 Å, R_{NO} = 1.4585 Å, R_{NN} = 1.0745 Å, indicating an extended NO bond length. This geometry corresponds to an activation energy of +63.5 kJ/mol, which is typical of all the other known azide structures.

FN_3

Calculations of the potential energy surfaces for FN_3, both ground and excited states, have been initiated to compliment the experimental studies of this system currently being undertaken at Rockwell Science Center. The energies and pathways for decomposition, and the prediction of emission/absorption wavelengths are being studied both theoretically and experimentally. Studies of the FN_3 system as a HEDM material and as a possible chemical source for $NF[a^1\Delta]$, with potential laser applications, are being pursued.

A detailed analysis of FN_3 has been carried out at geometries relevant to: a) the equilibrium ground $^1A'$ state, b) the transition state for decomposition to $NF[a^1\Delta]$ + $N_2[X^1\Sigma_g^+]$, and c) the region of singlet-triplet crossing. The details of these studies are outlined below:

a) Equilibrium Calculations

Ab initio theoretical calculations of the equilibrium structure and properties of fluorine azide (FN_3) have been performed using several standard basis sets and theoretical methods. Gradient-optimized structures and the corresponding harmonic vibrational frequencies have been calculated. Comparisons are made with the recent experimental results of Christen, Mack, Schatte, and Willner[2]. Good agreement with the experimental structure is found, with the correlated methods tending to correct the short SCF bond lengths. The harmonic vibrational frequencies are well described by MP2, except for the highest frequency mode, the terminal N-N stretch, which is predicted to be over 300 cm^{-1} too large. Systematic studies have shown MP2 vibrational frequencies are usually within 5% or so for small molecules.

b) Transition State Calculations

Calculations have been performed to locate the transition state for the decomposition of FN_3 into N_2 and NF. Transition state gradient optimizations were performed at the RHF/6-31G* and MP2/6-31G* levels of theory. To ensure that stationary points of the correct curvature have been found, harmonic vibrational frequencies have been computed for the transition structures. At the MP2/6-31G* optimized transition state, the RHF wavefunction is unstable with respect to a broken-symmetry UHF solution, and therefore the MP2 results may not be meaningful (for example, the extended central N-N bond length). Multireference calculations are required to reliably describe the effects of electron correlation on the transition state. Therefore, the transition state was also located using the 6-in-6 CAS MCSCF wavefunction. MP3 and coupled cluster calculations were also performed at the SCF geometries to assess the effects of a more complete treatment of electron correlation on the barrier height. These results suggest a barrier height of about

0.5 - 0.7 eV, including correction for vibrational zero-point motion.

c) Singlet-Triplet Splitting

The location of the FN_3 $^1A'$ - $^3A''$ crossing determines the singlet-triplet distribution of the $FN_3 \rightarrow N_2 + NF$ products. Experimental evidence[5] suggests that the crossing is on the product side of the barrier. *Ab initio* SCF calculations have therefore been performed to predict this crossing point from theory. These are UHF triplet calculations done at the RHF/6-31G* $^1A'$ optimized equilibrium and transition states. The UHF spin contamination was low, indicating that UHF is an acceptable level of theory for an initial approach to this problem. In order to locate the singlet-triplet crossing, the dissociative reaction path (intrinsic reaction coordinate) from the RHF/6-31G* $^1A'$ transition state was computed. At selected points on the reaction path, the singlet-triplet gap was calculated. We find the singlet- triplet crossing distance at N-N: 1.78Å, on the outside of he activation barrier of the ground state surface and close to the corresponding geometry predicted by Alexander and Dagdigian for HN_3.[6]

FNCO

The synthesis of fluorine isocyanate (FNCO) was first reported by Gholivand, et al[3] using photolysis of F-CO-N_3 in an argon matrix. This azide-like compound is predicted to be thermodynamically more stable than the isoelectronic FN_3 molecule. Our calculated equilibrium geometry is given in Table 1 which again indicates that the MP2/6-31G* level of theory gives good agreement with the experimentally determined structure. Harmonic vibrational frequencies are also well described at the MP2 level, except for the terminal C-O stretch.

Despite the greater thermodynamic stability of FNCO (ΔH_f^o ~ 0 kJ/mol), this molecule shows a similar dissociation pathway to that found for the halogen azides. We find the transition state at an FN-CO bond length of ~ 2.0 Å. The barrier height relative to the decomposition products $NF[a^1\Delta] + CO[X^1\Sigma^+]$ is calculated to be 0.76 eV at the GVB/6-31G* level of theory. RHF calculations are unreliable in this region since a multiconfiguration representation is required to achieve proper dissociation to the $a^1\Delta$ state of NF.

---

*Supported in part by AFAL under Contract F04611-86-C-0071.

[1] Tables of Interatomic Distances and Configurations in Molecules and Ions, L. E. Sutton, ed., Chemical Society, London (1985).

[2] D. Christen, H. G. Mack, G. Schatte and H. Willner, J. Am. Chem. Soc., 110, 707 (1988).

[3] K. Gholivand, H. Willner, D. B. Bielefeldt and A. Hans, Z. Naturforsch, 39b, 1211 (1984).

[4] D. E. Milligan and M. E. Jacox, J. Chem. Phys., 55, 3403 (1971).

[5] B. K. Winker, D. J. Benard and T. A. Seder, Quarterly Report No. 8, Contract F04611-86-C-0072, Rockwell International (1988).

[6] M. H. Alexander and P. J. Dagdigian, Proc. Second HEDM Conf., L. P. Davis and F. J. Wodarczyk, ed. (1988).

Table 1. Optimized Geometries of Azides

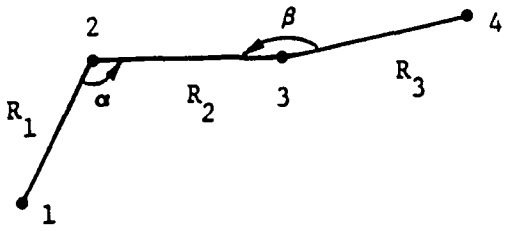

Compound	Theory	R_1(Å)	R_2(Å)	R_3(Å)	a (deg)	b (deg)
HN_3	SCF	1.0055	1.2381	1.0987	108.181	173.815
	MP2	1.0182	1.2502	1.1583	109.946	171.209
	Exp.[1]	1.012	1.240	1.134	*112.65*	*(180.0)*
FN_3	SCF	1.3820	1.2536	1.0995	104.315	174.108
	MP2	1.4309	1.2799	1.1521	103.765	171.803
	Exp.[2]	1.444	1.253	1.132	103.8	170.9
FNCO	SCF	1.3737	1.2387	1.1354	109.846	173.235
	MP2	1.4185	1.2622	1.1765	110.717	168.914
	Exp.[3]	1.39	1.28	1.18	114.0	(180.0)
a-N_2O_2	SCF	1.7574	1.2024	1.0844	103.966	179.506
	[MP2	1.5305	1.2272	1.1548	103.591	179.488]
	CISD	1.5817	1.2240	1.1072	102.867	179.344
FNBF	SCF	1.2993	1.2068	1.2871	180.000	180.000
	MP2	1.3394	1.2491	1.3069	154.650	169.291

( ) Assumed

[ ] ψ_0 is UHF unstable

azideabs.2/89

THEORETICAL STUDIES OF FN_3 CLUSTERS*

N. E. Brener, J. Callaway, N. R. Kestner, and H. Chen
Louisiana State University
Baton Rouge, Louisiana 70803

ABSTRACT

A new method of geometry optimization for large clusters of molecules, the simulated annealing procedure, has recently been developed. In this procedure, the molecular geometries are held fixed while inter-atomic potentials are used to describe the interaction between each pair of atoms in the cluster. In the case of FN_3 clusters, N-N, N-F, and F-F inter-atomic potentials are determined from atomic charges computed at the CISD level and from N_2-NF and NF-NF interactions computed at the MP2 level. This method, which simulates the process of gradually cooling the cluster from an initial high temperature, is fast and enables one to study clusters that are large enough to simulate the solid. Optimized geometries and average molecular volumes have been obtained for FN_3 clusters containing up to 12 molecules. In these calculations, the volume per molecule was found to quickly reach a nearly constant value as the size of the cluster increases. This converged value of the molecular volume has been used to compute the energy density of solid FN_3. In addition to the ground state (bent) molecular geometry, a linear molecular geometry has also been considered in the FN_3 cluster calculations.

---

*Supported by the Air Force Astronautics Laboratory (AFAL) under Contract F04611-87-K-0026.

THEORETICAL STUDIES OF FLUORINE AZIDE
In the Gas Phase and on Surfaces

by
Neil R. Kestner, Nathan Brener, and Joseph Callaway
Louisiana State University, Baton Rouge, LA 70803

Abstract

Theoretical studies of the electronic structure of fluorine azide will be discussed. The singlet and triplet surfaces will be explored at various levels of computation, for various size basis sets. Particular attention will be paid to the activation barrier and its position relative to the triplet state. In addition initial studies on the adsorption of fluorine and hydrogen azide on various ionic crystals will be presented.

Mechanisms of the Gas-Phase Decompositions of HN_3 and HNCO in the Presence of NO and O_2

Takayuki Fueno
Department of Chemistry, Faculty of Engineering Science, Osaka University, Toyonaka, Osaka 560, Japan

Reactions of $NH(^3\Sigma^-, ^1\Delta)$ with $NO(^2\pi)$ and $O_2(^3\Sigma_g^-)$ in the gas phase have been studied both theoretically and experimentally. The reactions are characterized by the initial formation of linear adducts, which are subject to unimolecular isomerizations and/or fragmentations in the ordinary pressure regime. Paths and pathways of the unimolecular processes have been investigated by ab initio SCF and CI procedures, and the fragmentation products have been identified experimentally.

I. Introduction

The $NH(^3\Sigma^-$ and $^1\Delta)$ radicals generated by either thermolysis or photolysis in the gas phase react readily with coexistent $NO(^2\pi)$ and $O_2(^3\Sigma_g^-)$ to give various types of fragmentation products. The overall reactions are considered to proceed via an intermediacy of the adduct radicals HN-NO and HN-OO, which subsequently will enter into isomerizations and/or fragmentations either with or without net activation barriers:

$$NH(^3\Sigma^-, ^1\Delta) + NO \longrightarrow \underset{1}{HN\text{-}NO} \longrightarrow \begin{cases} N_2O + H & (1a) \\ N_2 + OH & (1b) \end{cases}$$

$$NH(^3\Sigma^-, ^1\Delta) + O_2 \longrightarrow \underset{2}{HN\text{-}OO} \longrightarrow \begin{cases} NO + OH & (2a) \\ HNO + O & (2b) \end{cases}$$

Determinations of (i) the paths and pathways, (ii) the bimolecular rate constants and (iii) the fragmentation products of these bimolecular reactions are the primary purposes of this work.

II. Methods

Prior to experimental studies, the potential energy profiles for the reactions of NH with NO and O_2 have been scrutinized by ab initio calculations. The basis sets used are the conventional split-valence 4-31G or 6-31G functions augmented with one set each of polarization functions for every atom involved. The minimum-energy paths for reactions were traced by either the UHF SCF or RHF multiconfigurational(MC) SCF procedure, using the Gaussian 80 program package[1]. Geometries for the stable energy minima and the energy saddle points (transition states, TS) were all SCF-optimized. The transition states located as well as the relevant energy-minimum structures were then subjected to the multireference double-excitation (MRD) configuration-interaction(CI) computations [2] at the configurational space dimension of ca. 9000. The CI energies, which were extrapolated to the configuration-selection threshold $T \to 0$ hartree and subjected to the Langhoff-Davidson corrections, were adopted as the estimates of full CI values.

In the experimental studies, $NH(^3\Sigma^-)$ was generated by shock-heating of HN_3 (at 2200-2500 K) or HNCO (at 3500 K) diluted in Ar while $NH(^1\Delta)$, by photolysis (254 nm at 300 K) of the HN_3-Ar mixtures. The courses of reactions of NH with NO and O_2 were followed by monitoring the time-dependent absorption or emission of NH and OH or by mass-spectrometric determinations of stable final products. All experiments were carried out in the normal pressure region.

III. Results and Discussion

(A) Reactions with NO. The overall energy profiles calculated for the NH + NO system are shown in Fig. 1 [3]. It indicates that the initial association of $NH(^1\Delta)$ with NO has an exoergicity of ca. 430 kJ/mol and that the association product $HN\text{-}NO(^2A')$ should be collapsed spontaneously into N_2O + H (1a) and N_2 + OH (1b) in slight preference of channel (1a) over (1b). Mass-spectrometric analyses of the reaction mixtures have shown that N_2O is indeed a principal product, its quantum yield amounting to 0.70 in the limit of the initial molar fraction of NO $x = [NO]/([NO]+[HN_3]) \rightarrow 1$ (Fig. 2) [3]. Note that $NH(^1\Delta)$ reacts with the mother compound HN_3 as well essentially at the collision-controlled rate. The remaining fraction 0.30 is most likely to be due to channel (1b).

The possibility of the reaction channel (1b) was investigated for the case of $NH(^3\Sigma^-)$. Since the $NH(^3\Sigma^-)$ + NO system will also be led to $HN\text{-}NO(^2A')$ by the conical crossing of the doublet potential energy curves, the branching ratios for (1a) and (1b) will remain much the same as those for the case of $NH(^1\Delta)$. To confirm this, HNCO was shock-decomposed in the presence of excess NO and the reaction course was traced by monitoring the emission of OH (308 nm). The branching ratio for reaction (1b) was deduced to be 0.4 ± 0.1 (Fig. 3). The overall reaction proved to have a negative temperature dependence (E_a = -8.0 kJ/mol) (Fig. 4), in harmony with the theoretic1 prediction.

(B) Reactions with O_2. Reactions of $NH(^3\Sigma^-)$ with $O_2(^3\Sigma_g^-, ^1\Delta)$ are also expected to involve an initial association giving HN-OO. In the case of $O_2(^3\Sigma_g^-)$ as reaction partner, the intermediate adduct should uniquely be a <u>singlet</u> species of a closed-shell configuration $2(\tilde{X}^1A')$, which is calculated to be only 19 kJ/mol more stable than the reactant $NH(^3\Sigma^-)$ + $O_2(^3\Sigma_g^-)$. It will be thermally led to NO + OH through the following pathways:

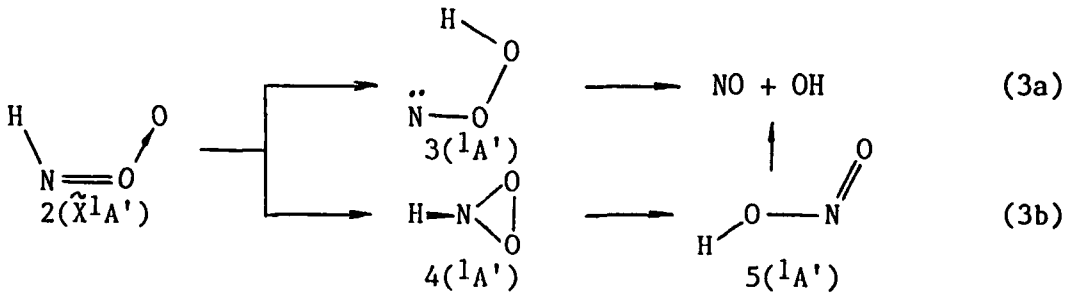

Intrinsic paths for the 1,3-hydrogen migration of 2 giving singlet hydroperoxynitrene (3) and the ring closure to give cyclic hydrogen nitroyl (4), both being yet unidentified entities, have been traced by the MC SCF procedure. Subsequent MRD-CI computations have shown that the activation barrier heights are 77 and 141 kJ/mol, respectively, against the initial $NH(^3\Sigma^-) + O_2(^3\Sigma_g^-)$ system (Fig. 5). Apparently, reaction (3a) is more favorable than reaction (3b). These results differ largely from those reported by Melius and Binkley [4], who seem to claim that the cyclic HNO_2 is the most probable precursor to NO + OH. Our calculated barrier height for (3a) is, however, still much too high as compared to the experimental activation energy (E_a = 19 kJ/mol) determined over the temperature range from 300 to 3500 K (Fig. 6).

Geometry optimizations and the MRD-CI energy calculations were worked out for both singlet and triplet HNOO diradicals in the $\pi\pi$(A'), $\pi\sigma$(A"), $\sigma\pi$ (A") and $\sigma\sigma$(A') states of the cis and trans structures. The lowest triplet state is $^3\pi\pi$, which is to be formed by the addition of $NH(^3\Sigma^-)$ to $O_2(^1\Delta)$ with an activation barrier of ca. 56 kJ/mol and which is to be collapsed into HNO and $O(^3P)$ with an additional activation energy of 9 kJ/mol.

Reaction between $NH(^1\Delta)$ and $O_2(^1\Delta)$ will be a concerted cycloaddition to give 4. 4 will readily be isomerized into nitrous acid (5) via "hydrogen nitroyl" $HNO_2(^1A_1)$, an intriguing planar symmetric isomer of 5.

References

[1] J. S. Binkley, R. A. Whiteside, R. Krishnan, R. Seeger, D. J. DeFrees, H. B. Schlegel, S. Topiol, L. R. Kahn and J. A. Pople, GAUSSIAN 80, QCPE No. 406.

[2] R. J. Buenker and R. A. Phillips, J. Mol. Struct. (THEOCHEM), 123, 291 (1985).

[3] T. Fueno, M. Fukuda and K. Yokoyama, Chem. Phys., 124, 265 (1988).

[4] C. F. Melius and J. B. Binkley, ACS Symp. Ser. 249 (1984); cited by W. Hack, H. Kurzke and H. Gg. Wagner, J. Chem. Soc., Faraday Trans. 2, 81, 949 (1985).

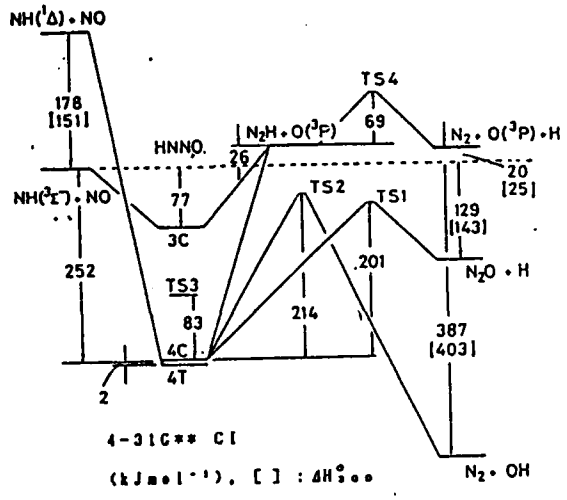

Fig. 1. Potential energy profiles of the HN-NO system [3].

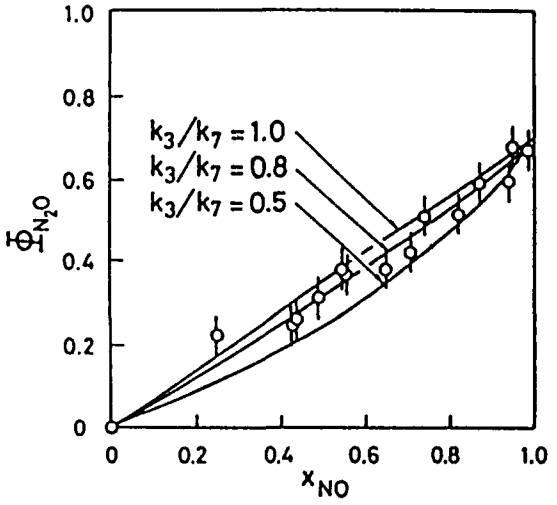

k_3 for $NH(^1\Delta) + NO$
k_7 for $NH(^1\Delta) + HN_3$

Fig. 2. Quantum yields of N_2O as the function of x(NO) [3].

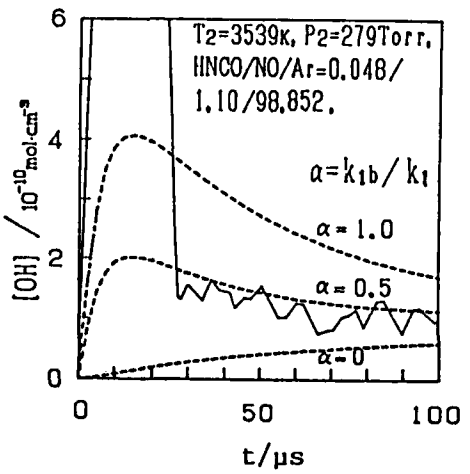

Fig. 3. Time history of [OH] in the reaction $NH(^3\Sigma^-) + NO \rightarrow N_2 + OH$.

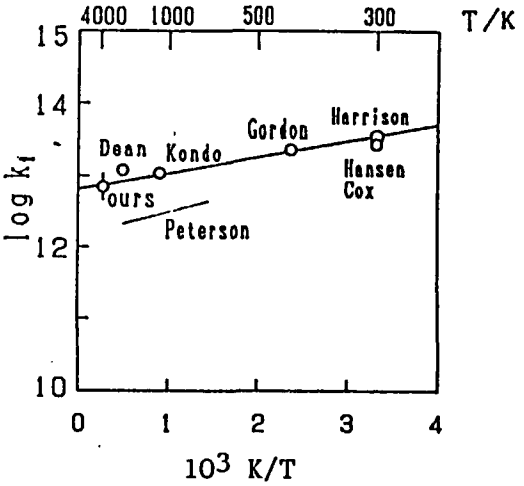

Fig. 4. Arrhenius plots of k for $NH(^3\Sigma^-) + NO \rightarrow N_2 + OH$.

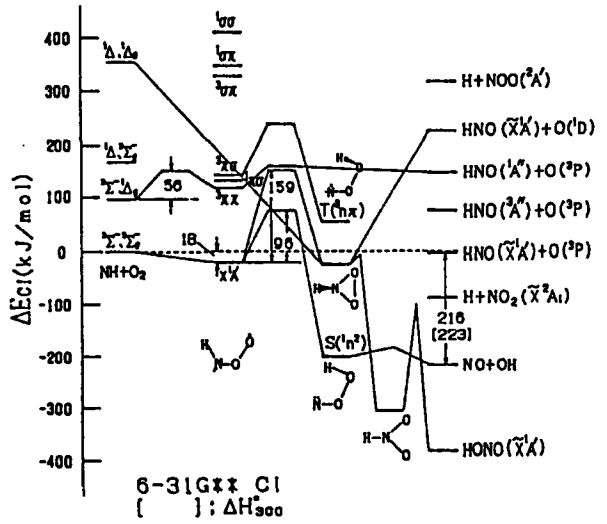

Fig. 5. Potential energy profiles for the HN-OO system.

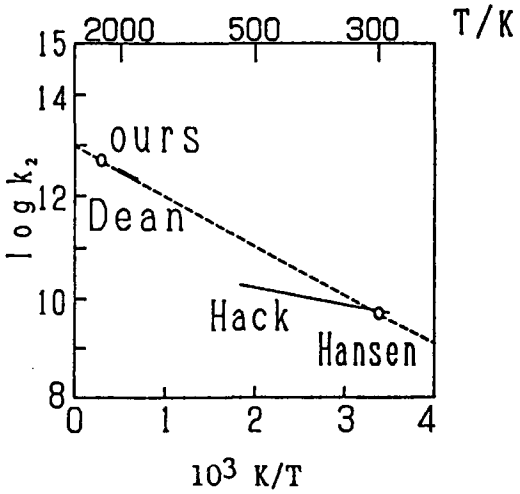

Fig. 6. Arrhenius plots of k for $NH(^3\Sigma^-) + O_2(^3\Sigma_g^-) \rightarrow NO + OH$

ISOCYANIC ACID AS A LASER FUEL

M. A. Chowdhury and D. J. Benard
Rockwell International Science Center
1049 Camino Dos Rios, Thousand Oaks, CA 91360

ABSTRACT

Spin and orbital constrained energetic reactions of NCO radicals with R atoms (R = C, O, P, N, F, Cl, Br, Si and B) have been investigated.The experiments were performed in a low-pressure flowtube by reacting F atoms with HNCO to generate the NCO radicals and with stable RHn to generate the R atoms. Chemiluminescence due to the NCO + R reactions was observed for each atom individually. Theses results indicate that in the cases of C, O and P atoms electronically excited NR* are generated. The NCO reactions are compared with the isoelectronic N_3 reactions and the similarities as well as differences are explained in terms of energetics and correlation rules based on spin and orbital symmetry. The yield of CN* was found to be the highest of the NR* species observed in this system. However,it was found (by absolute photometry) to be very low (1.4×10^{-3}% NCO s^{-1}). This may be due to inefficiency of the F + CH4 reaction as a C-atom source . Therefore an efficient C-atom source is essential for using the NCO + C reaction as the basis of a shortwavelength chemical laser.

EXPERIMENTAL STUDY OF DYNAMICAL PROCESSES ON HN_3 POTENTIAL ENERGY SURFACES: The H + N_3 Reaction, Photodissociation of HN_3, and Quenching of $NH(a^1\Delta)$ by N_2

Paul J. Dagdigian
Department of Chemistry
The Johns Hopkins University
Baltimore, MD 21218.

A progress report and preliminary results on three experiments which probe the dynamics of processes involving potential energy surfaces of HN_3. will be presented. These studies involve the determination of the internal state distribution of the products of various collisional processes, namely (1) the NH product from the H + N_3 chemical reaction, (2) the N_2 photofragment from the uv photodissociation of HN_3, and (3) the $NH(X^3\Sigma^-)$ from the electronic quenching of $NH(a^1\Delta)$ by N_2.

There are three possible NH products electronic states energetically accessible in the H + N_3 reaction:

$$H(^2S) + N_3(\tilde{X}\,^2\Pi_g) \rightarrow NH(X^3\Sigma^-) + N_2(X^1\Sigma g^+), \quad (1a)$$

$$\rightarrow NH(a^1\Delta) + N_2(X^1\Sigma g^+). \quad (1b)$$

$$\rightarrow NH(b^1\Sigma+) + N_2(X^1\Sigma g^+). \quad (1c)$$

Four potential energy surfaces arise from the interaction between H and N_3. If this reaction proceeds through the lowest surface, which includes the potential well corresponding to hydrazoic acid, $HN_3(\tilde{X}\,^1A')$, then we would expect preferential formation of $NH(a^1\Delta)$ through pathway (1b).

We shall report on our observations of $NH(a^1\Delta)$ product from the H + N_3 reaction. In our crossed beam study, hydrogen atoms are prepared in a supersonic microwave discharge source. Azide radicals are prepared by the reaction of fluorine atoms, produced in a CF_4/Ar microwave discharged flow, with hydrazoic acid. We found that our previously employed source of azide radicals, namely the thermal decomposition of lead azide, was not sufficiently intense, stable, or long-lived to be suitable for these

studies. The NH($a^1\Delta$) products are detected by laser fluorescence excitation in its $c^1\Pi \leftarrow a^1\Delta$ band system. We have thus far observed the v=0 and 1 vibrational levels through excitation of the (0,0) and (0,1) bands. The rotational energy distribution is found to be relatively cold, although we have not yet completely eliminated secondary rotational relaxation of the nascent products. Thus far, we have been unable to observe NH(a,v=2) products by excitation of the (0,2) band; however, based on recently measured NH c – a radiative transition probabilities,[1] the detection sensitivity for this level is considerably less than that for v=0 or 1.

We have also set up a time-of-flight mass spectrometer to determine the internal state distribution of $N_2(X^1\Sigma g^+)$ products from the uv photodissociation of HN_3 by resonant-enhanced multiphoton ionization (REMPI) detection:

$$HN_3(\tilde{X}\,^1A') + h\nu \rightarrow NH(a^1\Delta) + N_2(X^1\Sigma g^+), \qquad (2)$$

The calculations of M. H. Alexander[2] suggest that the N_2 photofragment could be formed with considerable rotational excitation We will report preliminary results for one-laser photodissociation/detection at the wavelength (283 nm) of the N_2 $a^1\Pi g \leftarrow X^1\Sigma g^+$ (1,0) band, which is used for the 2+2 REMPI process.

The *ab initio* calculations of Alexander[2] and the study of infrared multiphoton dissociation of HN_3 by King, Stephenson, and coworkers at NIST[3] suggest that there is a barrier of height 1000 – 1700 cm^{-1} in the spin-allowed decomposition channel, which yields NH($a^1\Delta$). This is also consistent with the recently measured small thermal rate constant for quenching of NH($a^1\Delta$) by N_2:[4]

$$NH(a^1\Delta) + N_2 \rightarrow NH(X^3\Sigma^-) + N_2, \qquad (3)$$

By contrast, the quenching of NH($a^1\Delta$) by CO has been found to be fast.[4]

In our laboratory, we have set up a crossed beam apparatus for the measurement of state-to-state inelastic cross sections involving small free radicals. Here, rotationally cold free radicals are prepared in their lowest rotational states by photolysis of a suitable precursor diluted in a seed gas at the tip of the nozzle of a pulsed beam. The free radical beam is crossed with a pulsed target beam, and the rotational states of the former are interrogated by laser fluorescence detection. We have previously used this

arrangement to determine rotationally inelastic cross sections for $NH_2(\tilde{X}^2B_1)$–He[5] and $NH(X^3\Sigma^-)$–Ar collisions.[6] More recently, we have prepared rotationally cold beams of $NH(a^1\Delta)$ by photolysis of HN_3. We have thus far measured pure rotationally inelastic cross sections for excitation out of the ground J=2 level of $NH(a^1\Delta)$ by various collision partners. Progress on the study of the quenching process, Eq. (3), will be reported at the meeting. By seeding both $NH(a^1\Delta)$ and the N_2 target in He seed gas, it is possible to reach a collision energy of 2000 cm^{-1}, which should be sufficient to overcome the expected barrier in the entrance channel.

---

1. H. H. Nelson, M. Hanratty, and J. R. Macdonald, work in progress at NRL, Washington, DC.
2. M. H. Alexander, abstract at this meeting.
3. B. R. Foy, M. P. Casassa, J. C. Stephenson, and D. S. King, J. Chem. Phys. **89**, 608 (1988); J. C. Stephenson, M. P. Casassa, and D. S. King, *ibid.* **89**, 1378 (1988); B. Foy, M. P. Casassa, J. C. Stephenson, and D. S. King, *ibid.* (submitted).
4. F. Freitag, F. Rohrer, and F. Stuhl, J. Phys. Chem. (submitted).
5. P. J. Dagdigian, J. Chem. Phys. **90**, XXXX (1989).
6. P. J. Dagdigian, J. Chem. Phys. **90**, XXXX (1989).

Chemiluminescent Reactions of Group VI Atoms with Azide Radicals

T. L. Henshaw, A. P. Ongstad and R. I. Lawconnell, Frank J. Seiler Research Laboratory, United States Air Force Academy, 80840–6528.

Recent work[1] has shown that the reactions between ground state atoms, R, and azide radicals , $N_3(X^2\Pi)$, are a useful way of generating chemiluminescence in the UV–VIS portions of the spectrum. In this study, we report on the kinetics of group VI atoms (R = O, S, Se) with azide radicals and the product distributions generated from the chemiluminescence of these reactions. A spectral code was generated to match calculated distributions with experimental values and obtain the vibrational distribution and rotational temperature for a particular set of conditions. For example, Figure 1 shows a typical spectrum of the $NS(B^2\Pi)$ chemiluminescence generated from the $S(^3P) + N_3(X^2\Pi)$ reaction, whose rate constant was determined to be $3.5 \pm 0.9 \times 10^{-11}$ cm^3s^{-1}. Superimposed on the experimental spectrum is the synthetic calculation (dashed lines). A best fit of experimental and calculated spectra to these data yielded a rotational temperature of 400 K and a vibrational distribution in accordance with the following

$v' =$	0	1	2	3	4
$f_v =$	.501	.176	.160	.004	.007

where f_v is the fractional vibrational population of level v'.

1). S. J. David and R. D. Coombe, J. Phys. Chem., 89, 5206 (1985).

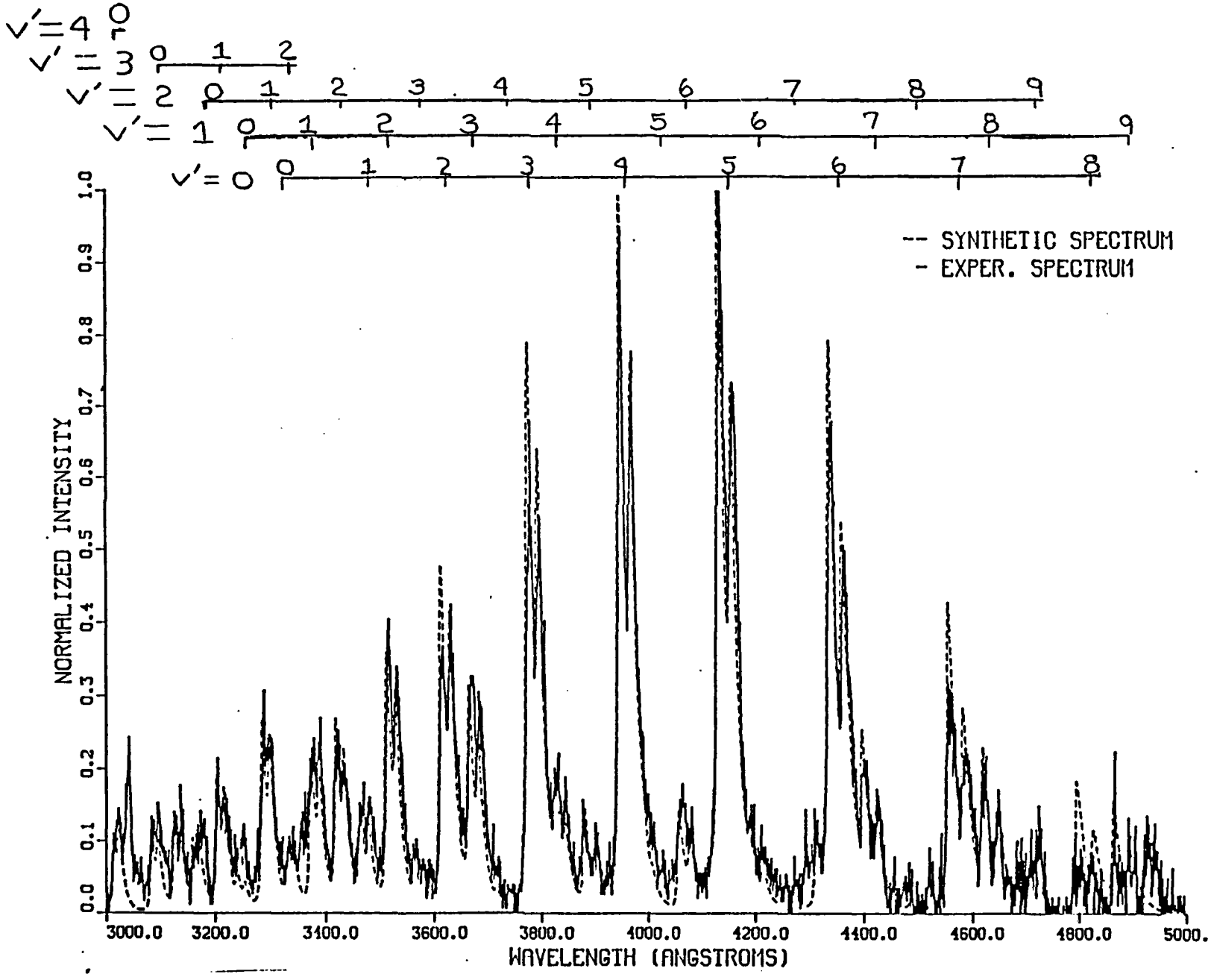

Figure 1. Comparison of experimental (–) and synthetic (- -) spectra of NS($B^2\Pi$). The experimental data was generated from the chemiluminescent S + N_3 reaction.

HYDRAZOIC ACID AS AN ANALYTICAL REAGENT

Donald H. Stedman and Mark R. Burkhardt

University of Denver Chemistry Department

Ultraviolet chemiluminescence (UVCL) at room temperature is very readily detectable at high sensitivity. There are relatively few reactions generating such chemiluminescence. In view of these facts, an analytical scheme based on UVCL is likely to be both sensitive and interference free. The reaction between oxygen atoms and azide radicals is one such reaction, the observed photons being NO gamma bands. In order to generate the azide radicals use is made of the fast reaction between fluorine atoms and HN_3. A mixture of F and O atoms produced by means of a microwave discharge in an air/CF_4 mixture is allowed to react with air containing a small concentration of HN_3 in a darkened reactor in front of a UV sensitive photomultiplier tube. This system is sensitive to HN_3 at trace levels down to parts per billion (ppb). It is not clear that detection of trace levels of HN_3 in air would ever be of itself interesting, were it not for the fact that it is possible to react any strong acid in the atmosphere with NaN_3 and thus liberate HN_3. The path which lead us from this concept to a functional system to measure the total acid gas concentration in the atmosphere will be described.

Electronic Excitation of Pb Atoms Following Detonation of Lead Azide*

I. Bar, A. Ben-Tov, Z. Ben-Porath, D. Heflinger, Y. Kaufman,
G. Miron, M. Sapir, Y. Tzuk and S. Rosenwaks

Department of Physics, Ben-Gurion University of the Negev
Beer-Sheva 84105, Israel

Abstract

The electronic excitation of Pb atoms in the gas phase, following the detonation of lead azide, Pb $(N_3)_2$, is monitored using chemiluminescence and laser induced fluorescence techniques. The detonation is initiated by either a laser pulse or an electrical spark. The fluid dynamics of the gaseous detonation products is monitored using high speed photography. The measurements indicate that as a result of the detonation, electronically excited N_2 is formed and a number of Pb states are preferentially populated by energy transfer from the N_2. The experimental study is accompanied by numerical modeling based on a coupled hydrodynamic-kinetic code. Both the experiments and the calculations indicate that high concentrations of excited, effectively long-lived Pb states are maintained as a result of radiation-trapping and that these states can be exploited to obtain laser transitions.

*The research is supported by Los Alamos National Laboratory under contract No. 9-X2D-1455G-1.

CHEMILUMINESCENT REACTIONS OF AZIDE RADICALS

W.J. Marinelli and W.J. Kessler
Physical Sciences Inc.
Research Park, P.O. Box 3100
Andover, MA 01810

We have examined a number of reactions involving the azide radical:

$$O + N_3 \rightarrow NO\ (A^2\Sigma) + N_2 \quad (1)$$

$$N + N_3 \rightarrow N_2\ (B^3\Pi_g) + N_2 \quad (2)$$

$$N_3 + N_3 \rightarrow N_2\ (B^3\Pi_g,\ A^3\Sigma_u^+,\ X^1\Sigma_g^+) + 2N_2 \quad (3)$$

The goal of this study is to explore the disposition of energy in the reactions and the propensity to produce electronically or highly vibrationally excited products. Reactions 1 and 2 are known to produce the electronically excited products shown. Reaction 3, by virtue of the high heat of formation of N_3 (4.4 eV), is capable of exciting N_2 electronic states within 1 eV of the dissociation limit. Little is known about the products of this reaction.

Two different methods were used to produce N_3 radicals in the gas phase. The first method, used to study the $O + N_3$ and $N + N_3$ reactions, involved the thermal pyrolysis of lead azide, $Pb(N_3)_2$. The lead azide was heated to about 200°C to evolve N_3 radicals. The N_3 radicals reacted with O-atoms and N-atoms in a discharge flow reactor. We report preliminary results on product vibrational temperature and distributions. These distributions show the NO(A) and $N_2(B)$ products present up to the exoergic limit. We were only able to estimate product yields due to our inability to determine exact N_3 densities at the time of these initial experiments. Our estimate of $N_2(B)$ production from reaction 2 is 70 percent of the yield of NO(A) from reaction 1. No direct production of $NO(B^2\Pi)$ or $N_2(A^3\Sigma_u^+)$ is observed from the reactions.

A second source of azide radicals was used to study the $N_3 + N_3$ disproportionation reaction. During these experiments we developed a new LIF technique to determine exact N_3 densities. This technique was simultaneously developed in the laboratories of Don Setser at Kansas State. Gas phase N_3 was produced by the $F + HN_3 \rightarrow HF + N_3$ reaction. This reaction is fast and, in excess HN_3,

quantitatively produces N_3 within the 1 cm mixing length of the HN_3 injector. The $N_3(A^2\Sigma_u^+, 000 - X^2\Pi_g, 000)$ band was excited via tunable radiation (272 nm) produced from anti-Stokes Raman shifting a Nd:YAG pumped frequency doubled dye laser. The resonance fluorescence was detected by a filtered PMT or a McPherson 270, 0.35 meter scanning monochromator. An $N_3(A \leftarrow X)$ spectrum is shown in Figure 1. Exact N_3 densities were determined by performing titrations when N_3 was generated under fast flow conditions. At low N_3 densities the $N_3 + N_3$ reaction is slow, thus there is no N_3 decay prior to LIF detection of the radicals. This allows us to absolutely calibrate the LIF signal with the N_3 density. At higher N_3 densities the $N_3 + N_3$ reaction proceeds at a much faster rate. The N_3 disproportionation rate coefficient was measured by varying the $N_3 + N_3$ reaction time prior to LIF detection of the radicals. The reaction time was varied by changing the position of the HN_3 sliding injector relative to the optical detection point. A plot of $1/[N_3]$ versus HN_3 injector distance from detection region is shown in Figure 2. The reaction displayed characteristic second-order kinetics under all conditions examined. A rate coefficient of 2.4×10^{-12} cm^3 $molecule^{-1}$ s^{-1} was obtained from the measurements. No excited electronic states of N_2 were observed from the reaction. Upper bounds were placed on $N_2(A)$ and $N_2(B)$ product yields based on chemiluminescence spectra.

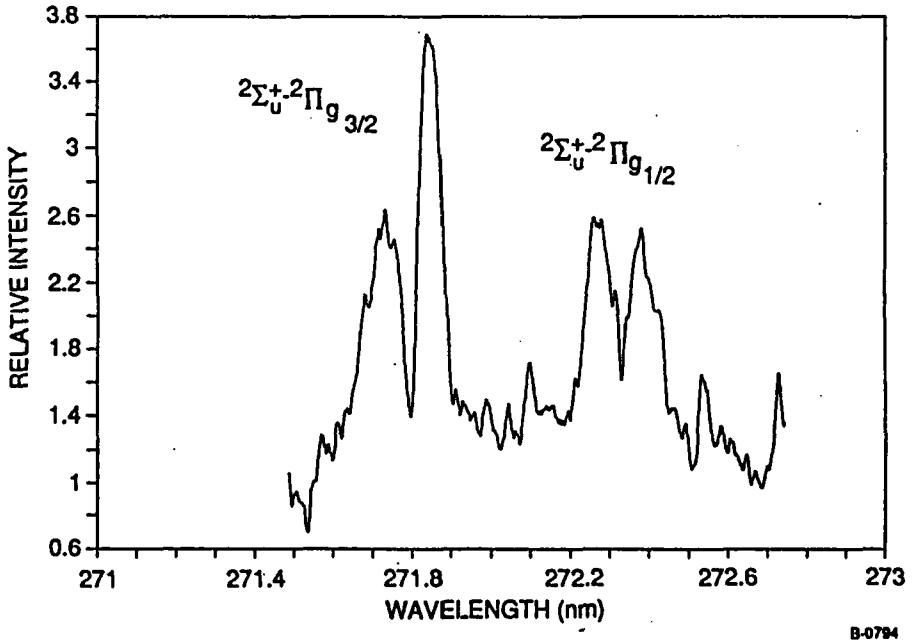

Figure 1. N_3 LIF Spectrum of the $(A^2\Sigma_u^+, 000 \leftarrow X^2\Pi_g, 000)$ band. N_3 was produced via the F + HN_3 reaction.

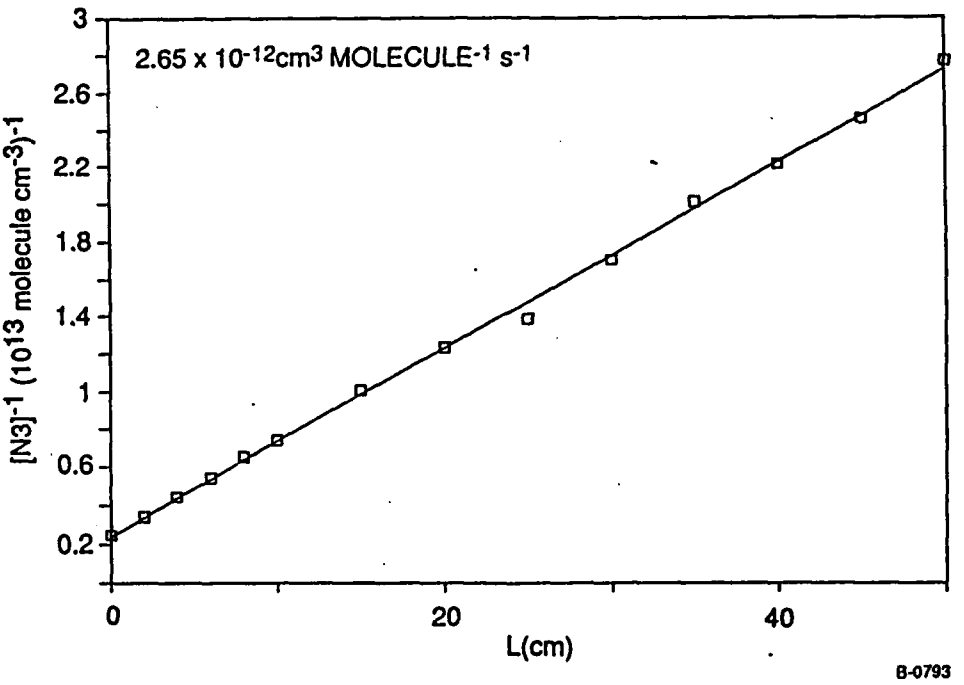

Figure 2. Plot of N_3 radical decay due to bimolecular recombination versus HN_3 injector position.

The apparent specificity of reactions 1 and 2 to form the observed products can not be rationalized on the basis of adiabatic correlation diagrams. Assuming the reactions proceed through C_s symmetry, all of the energetically accessible triplet states in N_2 may be formed by reaction 2. Production of ground state N_2 is spin-forbidden. All states of NO up to the exoergic limit may be formed from reaction 1. The slow rate for reaction 3 provides indirect evidence for the existence of a complex intermediate. Randomization of energy in the complex would explain the apparent formation of only ground state N_2 molecules as products.

Our present efforts in azide chemistry are concentrated on understanding the rate and product yields for the reaction of O-atoms with N_3 (reaction 1). Of particular interest is the yield of $NO(A^2\Pi)$. Many of our previous observations on the reaction of N-atoms with N_3 are referenced to the chemiluminescence yield of NO(A) from reaction 1. We believe an accurate measurement of these quantities will enable us to quantitatively relate many of our previous measurements and provide a better understanding of azide chemistry.

This work is sponsored by Los Alamos National Laboratories for SDIO/IST.

$NO(A \rightarrow X)$ and $N_2(C \rightarrow B)$ Laser Experiments

M. D. Burrows, R. F. Shea, and G. W. York
Los Alamos National Laboratory
Los Alamos, NM 87545

We have recently demonstrated in our laboratory what appears to be weak $NO(A \rightarrow X)$ lasing pumped by energy transfer from $N_2(A)$. The $NO(A \rightarrow X)$ lasing is particularly weak when compared to our observed $N_2(C \rightarrow B)$ lasing at 406 nm at intrinsic efficiencies of nearly 3%. Further experiments are in progress to verify NO lasing action and these results will be presented. In order to calibrate the NO(A) densities obtained by electron-beam pumping via measured relative $N_2(C \rightarrow B)$ and $NO(A \rightarrow X)$ fluorescence intensities, we have lased $N_2[(C,O) \rightarrow (B,v'' = 1,2,3)]$ at 358, 380, and 406 nm, respectively. At moderate pump levels (35 kW/cc electron-beam power deposition) and using a high reflectivity cavity at 358 to 406 nm, we observe the sequential lasing at 358 and 406 nm displayed in Fig. 1. In spite of a high stimulated emission cross section for the 380-nm transition, which shares the same upper laser level with the observed 358- and 406-nm laser lines, lasing at 380 nm is not observed. At stronger pump levels (90 kW/cc), weak 380-nm lasing is observed between the two strong 358- and 406-nm pulses displayed in Fig. 2. This anomalously weak lasing action at 380 nm is attributed to "up conversion" of $N_2(A,v' = 8)$ to $N_2(A,v' = 10)$ by collisions with $N_2(X,v = 1)$, both of which are plentiful in our electron-beam environment, followed by rapid conversion of $N_2(A,v = 10)$ to $N_2(B,v = 2)$. The energy difference between $N_2(A,v = 10)$ and $N_2(B,v = 2)$ is only 136 cm^{-1}, and the additional $N_2(B,v = 2)$ produced reduces the available gain at 380 nm.

When one of the 358- to 406-nm high reflectivity mirrors is replaced by one that is 80% R at 406 nm, 20% R at 380 nm, and 15% R at 358 nm, a 406-nm lasing pulse shape nearly identical to that in Fig. 2 is observed. For a 1-inch diameter laser aperture, pulse energies of ~200 mJ/cm^2 were observed. This is equivalent to a total energy across the full electron-beam-pumped aperture of 10 x 10 cm of 20 J at an intrinsic efficiency of nearly 3%, in spite of the fact that nearly 40% of the pump energy is unused due to cavity build-up effects. By comparison, XeF operation in the same electron-beam-pumped laser yields intrinsic efficiencies of 1.5%.

The addition of a few torr of H_2 to our $N_2(C \rightarrow B)$ laser gas mixes significantly increases the cavity decay time for 406-nm lasing by removing sources of direct $N_2(B)$ production. This effect is consistent with measured ion-molecule reaction rates and has allowed us to better understand the detailed kinetics of Ar^* and, therefore, $N_2(C)$ formation. Preliminary kinetic results indicate an $N_2(C,O)$ formation efficiency of at least 50%.

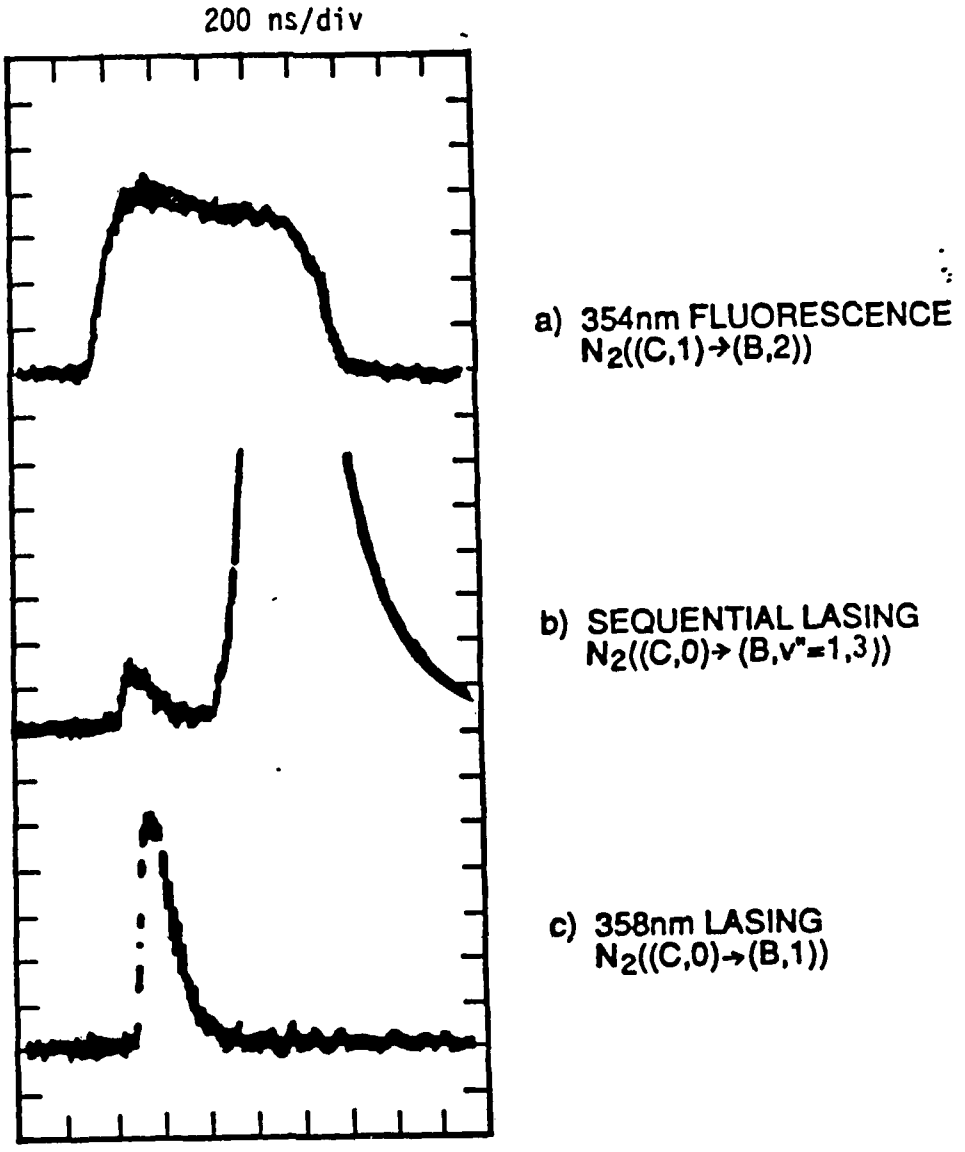

Figure 1. Sequential $N_2((C,0) \rightarrow (B,v'=1,3))$ lasing from electron-beam excitation (~35 kW/cc) of 1250 torr Argon + 100 torr N_2 using a high reflectivity cavity at 358 to 406 nm. The same oscilloscope timing trigger pulse was employed in all traces. The 354 nm fluorescence pulse in (a) accurately reflects the electron-beam current pulse of approximately 1 usec duration. Trace (b) displays sequential lasing at 358 and 406 nm, while trace (c) displays the 358 nm lasing pulse separated from the total lasing pulse using an interference filter.

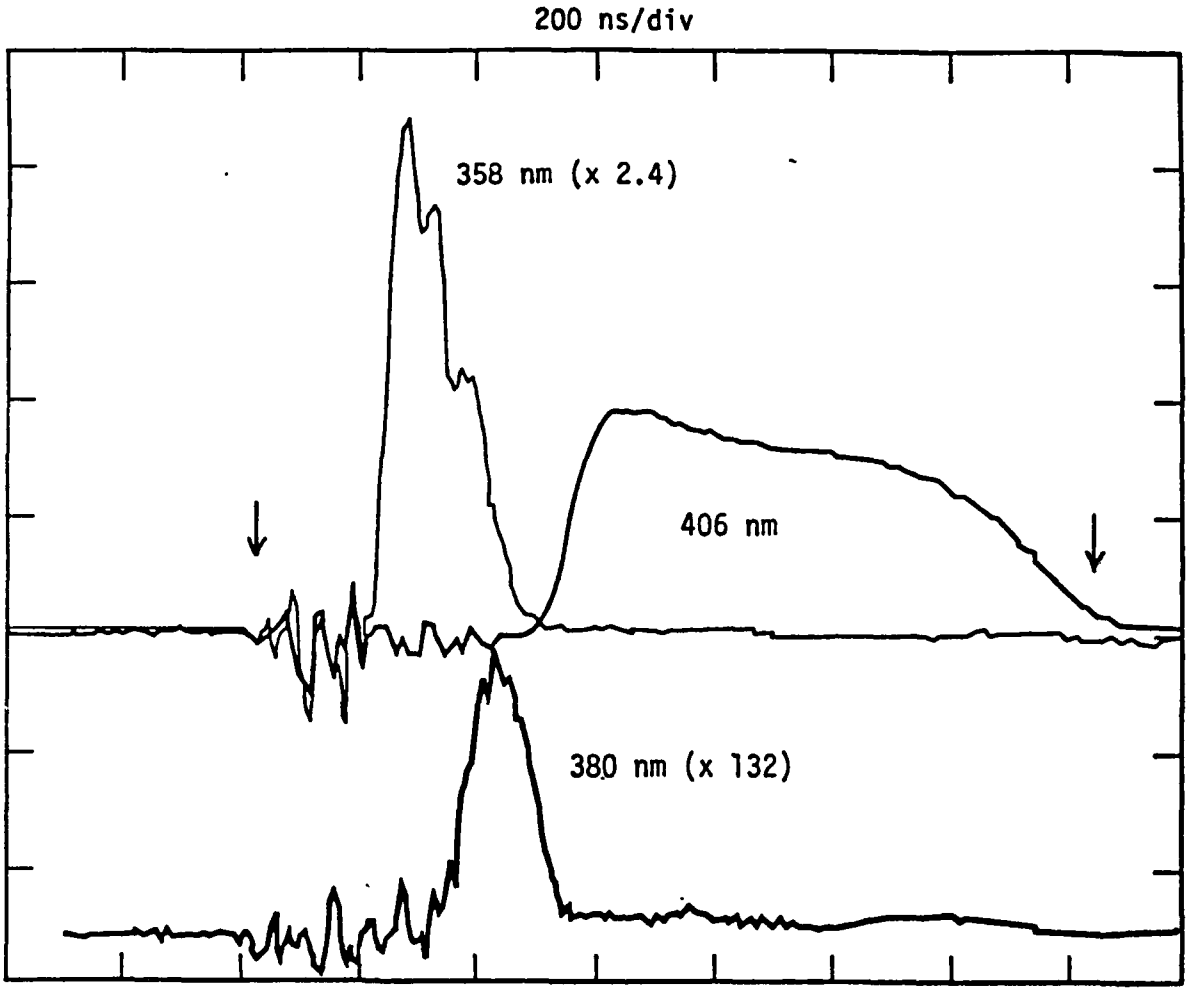

Figure 2. Sequential $N_2((C,0) \rightarrow (B,v'=1,2,3))$ lasing from electron-beam excitation (~90 kW/cc) of mixtures of 1450 torr Argon + 100 torr N_2 using the same high reflectivity cavity as in Figure 1. Weak lasing at 380 nm is observed to occur between the two strong lasing pulses at 358 and 406 nm. The temporal extent of the electron-beam pulse, including rise and fall times, is indicated by the vertical arrows.